JAERI-M
89-217

A MODEL OF L-H TRANSITION

December 1989

Hiroshi AIKAWA

日本原子力研究所
Japan Atomic Energy Research Institute

JAERI-M レポートは，日本原子力研究所が不定期に公刊している研究報告書です。
入手の問合わせは，日本原子力研究所技術情報部情報資料課（〒319—11 茨城県那珂郡東海村）あて，お申しこしください。なお，このほかに財団法人原子力弘済会資料センター（〒319-11 茨城県那珂郡東海村日本原子力研究所内）で複写による実費頒布をおこなっております。

JAERI-M reports are issued irregularly.
Inquiries about availability of the reports should be addressed to Information Division, Department of Technical Information, Japan Atomic Energy Research Institute, Tokai-mura, Naka-gun, Ibaraki-ken 319-11, Japan.

編集兼発行　日本原子力研究所
印　　刷　山田軽印刷所

JAERI-M 89-217

A Model of L-H Transition

Hiroshi AIKAWA

Department of Thermonuclear Fusion Research
Naka Fusion Research Establishment
Japan Atomic Energy Research Institute
Naka-machi, Naka-gun, Ibaraki-ken

(Received November 28, 1989)

A model of L-H transition in a tokamak plasma is presented. In the theory of the dissipative drift wave turbulence, the condition of $k_\perp^2\rho_i^2 \gtrless 1$ ($k_\perp$: wave vector normal to the magnetic field, ρ_i: ion Larmer radius evaluated by electron temperature) makes the theoretical procedures change from the fluid type to the kinetic one as $k_\perp\rho_i$ grows over unity. This fact leads the diffusion coefficient induced by this instability to utterly different dependence of plasma parameters (especially electron temperature (T_e) dependence changes from $T_e^{5/6}$ to T_e^{-2} as $k_\perp^2\rho_i^2$ changes from the value less than unity to the value more than unity). It is shown in the present paper that L-H transition can be induced by this change of plasma parameter dependence of the diffusion coefficient, and the threshold value of electron temperature is also presented. This model, using the radial profiles of electron density and temperature near the plasma circumference obtained by the experiment of ASDEX, shows a good explanation of L-H transition. The various characteristics of H-mode, having been obtained by the various tokamak machines with the various conditions, are discussed and also explained consistently.

Keywords: L-mode, H-mode, Model, Transition, Tokamak, Plasma

JAERI－M 89－217

Ｌ－Ｈ　遷移モデル

日本原子力研究所那珂研究所核融合研究部
相川　裕史

（1989年11月28日受理）

トカマク・プラズマにおけるＬ－Ｈ遷移に対する１つのモデルが提案されている。それは散逸性ドリフト波乱流理論において$k_\perp^2 \rho_i^2 \gtrless 1$（$k_\perp$：磁場に垂直方向の波数ベクトル，$\rho_i$：電子温度で評価したイオン・ラーモア半径）を境にして理論的取扱いが流体タイプ（$k_\perp^2 \rho_i^2 < 1$）から軌動論的（$k_\perp^2 \rho_i^2 > 1$）に変化し，それによって拡散係数のプラズマ・パラメータ依存性が大きく異なることから（特に電子温度（T_e）依存性は$k_\perp^2 \rho_i^2$が１より低い値から１より高い値に変化するにつれて，$T_e^{5/6}$からT_e^{-2}へと大きく変化する。），Ｌ－Ｈ遷移が起り得ることを示した。このモデルから求められる電子温度の閾値を示した。また，このモデルを基に，プラズマ周辺での電子密度と電子温度分布のＡＳＤＥＸによる実験データにあてはめてみたところ，大変良い一致を示した。また，その他の装置のこれまでのさまざまな実験結果とも比較検討を行い，ほとんどの実験結果を説明し得ることを示した。

那珂研究所：〒311－01　茨城県那珂郡那珂町大字向山801－1

Contents

目　　次

1. Introduction

Since the discovery of a good confinement mode (so called H-mode) by ASDEX[1] in 1982, L-H transition phenomenon in Tokamak has still remained an unsolved important problem no matter how considerable efforts have been spent on both the experimental and theoretical aspects[1~3].

The important point to remark is that H-mode transport in the vicinity of a plasma edge is highly improved enough to lead the improvement of the inner transport[4]. Concerning to the outer transport near the plasma circumference, the research has been relatively left behind until the discovery of H-mode because the complicated circumstances related to the plasma boundary make the study difficult while the global confinement time is expected to be determined by the inner part of a plasma column which holds a considerable amount of a plasma kinetic energy.

The footlighted vital question relating to the H-mode mechanism is what type of instability is dominant or relevant to the diffusion in the outer region at L-H transition. The dominant diffusion should be expected to be caused by a certain specific type of instability, not by the combination of some several instabilities because the clear drastic change at L-H transition may be unlikely produced by the conditions required by several instabilities, each of which has generally complicated parameter dependences. The common type of instability may be preferable because L-H transition occurs comparatively easily on several machines. Therefore, of the various theories related to the outer transport, the dissipative drift wave instability is the most ordinary conceivable condidate that may dominate the diffusion of the outer region in L-H transition. This instability, however, has an unfavorable dependence of electron temperature (T_e) on the diffusion coefficient (D) ($D \propto T_e^{5/6}$), because the experimental results indicate that when T_e increases over a certain threshold value (T_{th}), the diffusion suddenly decreases and the plasma turns to H-mode. This fact leads the author to the hypothesis that above T_{th}, the diffusion may be dominated by some instability whose dependence of D on T_e should be $T_e^{-n}(n>0)$, while below T_{th}, D may allow the form of $T_e^{m}(m\geq 0)$.

According to Kadomtsev and Pogutse[5], the diffusion coefficient of the dissipative drift wave turbulence in case of $k_\perp^2\rho_i^2 < 1$ ($k_\perp$: wave number normal to magnetic field, ρ_i: ion Larmor radius evaluated by electron temperature) is given as

$$D_{KP} = \frac{\nu_e^{1/3}(\rho_e v_e)^{4/3}(1+\frac{T_i}{T_e})^{1/3}}{(r_n\theta)^{2/3}(\Omega_i\Omega_e)^{1/3}} \tag{1}$$

where

$$r_n^{-1} = \left| \frac{d \ln n_e}{d r} \right| \tag{2}$$

$$\theta = \frac{r\, r_n}{B} \left| \frac{d}{dr} \frac{B_\theta}{r} \right| \tag{3}$$

ν_e: electron collision frequency, ρ_e: electron Larmor radius, v_e: electron thermal velocity, T_i: ion temperature, T_e: electron temperature, r_n: density gradient length, n_e: electron density, θ: shear parameter, B: toroidal magnetic field, B_θ: poloidal magnetic field, Ω_i: ion cyclotron frequency, and Ω_e: electron cyclotron frequency.

This equation indicates $D_{KP} \propto T_e^{5/6}$. When $k_\perp^2\rho_i^2 > 1$ (in other words, T_e increases), on the other hand, the diffusion due to this instability is known to reduce to a small value enough to a safety level and has been overlooked as one of the safe cases, only treated as a compromized form of the pseudo-classical diffusion. The author would like to throw a light to this case, because the most desired diffusion now is the safest one when the plasma turns to H-mode.

Using the simple and clear physical analysis, Kadomtsev and Pogutse[5] approximately obtain the criterion of $k_\perp^2\rho_i^2 \geq 1$ where the diffusion due to the dissipative drift wave instability becomes dominant, with the form of

$$S \equiv \frac{\lambda_e \rho_i}{a^2} \geq \sqrt{\frac{\rho_i}{a}} \Big/ \theta \tag{4}$$

where S: collisional parameter, λ_e: electron mean free length, a: plasma minor radius. This equation can be rewritten as

$$T_e \geq \text{const.} \frac{a^{2/3} B^{2/9} Z_{eff}^{4/9} n_e^{4/9}}{\theta^{4/9} A^{1/9}} \quad (\equiv T_{th}^{approx.}) \tag{5}$$

where Z_{eff}: effective ion charge number, and A: ion mass number. The equation (5) indicates that as Te increases from $T_e < T_{th}^{approx}$ to $T_e > T_{th}^{approx}$, $k_\perp^2 \rho_i^2$ increases from the value below unity to the value above unity and the diffusion coefficient turns from the dangerously large D_{KP} to a safely small one which is to be deduced in the following section. This picture matches the desired one.

In the following sections, the possibility that the above-described physical picture matches the situation is investigated from the various aspects. In the next section, the diffusion coefficients in case of both $k_\perp^2 \rho_i^2 \gtrless 1$ are obtained to induce T_e threshold which is compared with the experimental results. In the third section, the experimentally obtained n_e and T_e radial profiles near the plasma edge by ASDEX are used to obtain the diffusion coefficient due to the dissipative drift wave turbulence and the differences between L and H mode are discussed. In the fourth section, the mechanism of L-H transition is investigated based on the assumption of a small T_e disturbance as a trigger of the transition. In the fifth section, various characteristic features of H-mode are compared between the experimental results and the model. In the last section, the results are summarized.

2. Motivation

As described in the previous section, the diffusion coefficient in case of $k_\perp^2\rho_i^2<1$ is given as Eq.(1), while, in case of $k_\perp^2\rho_i^2>1$ (high T_e), the theoretical treatment moves from the fluid type to the kinetic one, so that Eq.(1) cannot be used.

In case of $k_\perp^2\rho_i^2>1$, Kadomtsev and Pagutse[5] also gives the growing rate (γ) and localijation length (X) as

$$\gamma \sim \omega_{pe}^{*}\sqrt{\delta} \tag{6}$$

$$X \lesssim \rho_i\sqrt{\delta} \tag{7}$$

where

$$\delta = \frac{1}{m\theta^2}\sqrt{\frac{m_e}{m_i}}\Big/ S \tag{8}$$

$$m = \sqrt{a/x} \tag{9}$$

$$\omega_{pe}^{*} = \omega^{*}(1 + \eta_e) \tag{10}$$

m_e: electron mass, m_i: ion mass, $\eta_e=r_n/r_T$, $r_T^{-1}=\left|\frac{d \ln T_e}{d r}\right|$ and ω^*: electron diamagnetic frequency.

Therefore, the diffusion coefficient, taken into account of the maximum value of $X=\rho_i\sqrt{\delta}$ and the ordinary linear treatment of the instability, is given to be

$$D_H = \gamma X^2 = \frac{\rho_e\, \nu_e^{5/3}\, a^3\, \Omega_i^{1/2}(1+\eta_e)}{\theta^{10/3}\, r_n\, r\, \Omega_e^{7/6}} \tag{11}$$

which has a T_e-dependence of T_e^{-2}.

Now, the whole region of $k_\perp^2\rho_i^2$ is covered by Eq.(1) and Eq.(11) in the dissipative drift wave turbulence. That is, in case of $k_\perp^2\rho_i^2<1$ (in case of low T_e), Eq.(1) is used and in case of $k_\perp^2\rho_i^2>1$ (in case of high T_e), Eq.(11) is used. At $k_\perp^2\rho_i^2=1$, Eq.(1) and Eq.(11) should represent the same value and over $k_\perp^2\rho_i^2=1$, Eq.(11) should be lower than Eq.(1). Therefore, to obtain the threshold T_{th} which classifies the region where Eq.(11) can be used, we set Eq.(1) and Eq.(11) as follows;

$$D_H < D_{KP} \tag{12}$$

This inequality equation can be easily rewritten to be

$$T_e > \text{const.} \frac{Z_{eff}^{8/17} n_e^{8/17} a^{18/17} B^{2/17} (1+\eta_e)^{6/17}}{A^{5/17} \theta^{16/17} r_n^{2/17} r^{6/17} (1+\frac{T_i}{T_e})^{2/17}} \ (\equiv T_{th}). \tag{13}$$

where we take the electron-ion collision frequency as ν_e, but the question as to what the dominant collision is still remains ambiguous. It should be noted here that Eq.(13) should be physically identical with Eq.(5) which is induced approximately from the viewpoint of the physical insight though the parameter dependences are a little different from each other.

For the practical use of Eq.(13), a few assumptions are taken as $\ln\Lambda=15$, and $j \propto j_o(1-\frac{r^2}{a^2})$. Then, T_{th} can be rewritten as

$$T_{th} = 1.66\times10^{-2} \frac{Z_{eff}^{8/17} n_e^{8/17} a^{82/17} B^{18/17} (1+\eta_e)^{6/17}}{A^{5/17} Ip^{16/17} r_n^{18/17} r^{38/17} (1+\frac{T_i}{T_e})^{2/17}} \tag{14}$$

where the units are $n_e(m^{-3})$, a(m), B(T), Ip(A), r_n(m), r(m) and T_{th}(eV).

As described in the previous section, the motivation is that T_{th} given by Eq.(14) be the threshold of L-H transition. Equation (14) gives approximately the linear dependence of B, consistent with the experimental result[6]. And Equation (14) gives $A^{-5/17}$-dependence, not unfavorable with the experiment[7]. Equation (13) also indicate $\theta^{-16/17}$-dependence which is also favorable with the experimental result[8]. The density dependence is a little ambiguous because Eq.(14) superficially gives $n_e^{8/17}$-dependence but r_n contains n_e so that T_{th} is linear with $n_e^{-10/17}$, though we had not yet convincing data as to what role the density gradient (dn_e/dr), which is included in r_n, may take at the density scanning. And Eq.(14) gives approximately the linear dependence of B/Ip which gives the favorable status to the experimental results by JFT-2M[7], but superficially contradicting with DIII-D results[9], though n_e, dn_e/dr, and j-profile etc. cannot be proved unchanged during Ip-scan experiment. More precise experiment

should be needed to determine the dependences.

As mentioned above, many favorable features on the parameter dependences can be shown by Eq.(14). In the next section, more detailed comparison with the experiment is tried with the use of ASDEX-data.

3. Comparison with Experimental Results

To investigate the validity of the model described in the previous section, it would be more helpful to apply it to the data obtained by the actual experiment. But, the calculation of D_{KP}, D_H, S and $\sqrt{\rho_i/a}/\theta$ needs a complete data set of plasma parameters (n_e, T_e, T_i, j, etc.), though it is not so easy for the present experimental situation. Therefore, here, ASDEX data[10], which is comparatively set in good order for our purpose, is used as a main data with additional few assumptions of $T_i=T_e$, Z_{eff}=const.(=2), and $j \propto (1-r^2/a^2)$. Of those assumptions, $T_i=T_e$ makes no problem because T_i only enters in D_{KP} in the term of $(1+T_i/T_e)^{1/3}$ which is comparatively insensitive of T_i values because of a-third power. Z_{eff} is also insensitive to D_{KP} by the same reason with T_i-case, while it is comparatively sensitive to D_H because Z_{eff} enter into the term of $\nu_e^{*5/3}$. As for j-profile, it has significant effect on D_H because j-profile is contained in θ in the form of $\theta^{10/3}$. It should be noted here that these ambiguities, which are to be investigated in the future experiment, cannot be helped included in the present analysis.

The calculated results of S and $\sqrt{\rho_i/a}/\theta$ are shown in Fig. 1, which tells that S is found to be much lower than $\sqrt{\rho_i/a}/\theta$ in OH and L-mode plasma while in H-mode plasma, S is found to exceed the value $\sqrt{\rho_i/a}/\theta$ at $\Delta r \simeq -3.6$cm. This fact means that in OH and L-mode plasma, $k_\perp^2\rho_i^2<1$, and the diffusion by the dissipative drift wave instabilidy is dominated by D_{KP} at the circumference of the plasma, while in H-mode plasma, $k_\perp^2\rho_i^2$ grows over unity and the diffusion by the dissipative drift wave instability is substituted by D_H in the inner region ($\Delta r \lesssim -3.6$cm), though the outer region (near the plasma edge, $0 \geq \Delta r > -3.6$cm) is still dominated by D_{KP}. This fact matches the expected one. To confirm this expectation, D_{KP} and D_H are calculated and shown in Fig. 2. In OH and L-mode plasma, D_H is found exceedingly higher than D_{KP}, which tells that D_{KP} should be adopted in these cases, while in H-mode plasma, D_H is higher than D_{KP} near the plasma edge, similar as in case of OH and L-mode, but D_H becomes equal to D_{KP} around $\Delta r \simeq -3$cm (this position differs a little from the position determined by $S=\sqrt{\rho_i/a}/\theta$ of Fig. 1(c), whose difference should be explained from that S-and-$\sqrt{\rho_i/a}/\theta$ theory is an approximate one), beyond which D_H becomes much lower than D_{KP}. Therefore, in H-mode plasma, the diffusion by the dissipative drift wave is

determined by D_{KP} in the outer region ($0 \geq \Delta r \gtrsim -3$cm), while it is determined by D_H in the inner region ($\Delta r \lesssim -3$cm). The diffusion coefficient D_H of H-mode in the inner region shows a very low value. This fact raises up the possibility that the diffusion due to some other competing modes of instabilities, besides the dissipative drift wave, should be taken into consideration. As most possible candidates, the drift wave theory tells us two modes, the collisionless drift wave or the dissipative trapped electron mode concerning to the plasma parameters considered here. The contribition by the collisionless drift wave in case of H-mode in Fig. 2(c) is found considerably smaller than D_H in the region of $-5\text{cm} \leq \Delta r \leq -3$cm because of high shear parameter, while the dissipative trapped electron mode cannot be ignored and it steeply grows inwardly from around $\Delta r \simeq -3$cm. The behavior is also shown in Fig. 2(c). Therefore, the totally added diffusion coefficient of H-mode plasma shows a deep dip of width ~1.5cm around $\Delta r \simeq -3.4$cm, as shown in Fig. 2(c).

This interesting reuslt tells us that the diffusion or the heat flow of H-mode plasma shown in Fig. 2(c) stops at this deep dip, as though it works like a kind of an adiabatic layer. In case of L-mode plasma in Fig. 2(b), the contributions of the collisionless drift wave and the dissipative trapped electron mode are found less than one-severalth of D_{KP} so that D_{KP} may be treated as a dominant mode, though the possibility that any other mode may dominate or take some considerable contribution in the region with the plasma parameters considered here is still an open question, and the precise analysis and experiment should be expected in the future.

Now, let's try to draw a picture of the L-to-H transition behavior. At first, the plasma is assumed to stay in L-state of Fig. 2(b), and then T_e is assumed to go up by some cause as NB injection or ECH heating or Sawtooth crash. Then $k_\perp \rho_i$ increases to exceed unity and the dissipative drift wave instability enters the kinetic region and the diffusion turns from D_{KP} to D_H, with the value of the diffusion coefficient getting much smaller and smaller, and D_{TE} (due to the dissipative trapped electron mode) grows much larger than D_H to form the deep dip of Fig. 2(c). In this picture, only T_e is adopted as a variable with the other parameters fixed. But the actual situation tells that the other parameters changes largely at the transition, especially the density profile changes to a flat profile from an ordinary gradient one. Here, let's set the discussion on some fixed

position and observe the behavior of D_{KP} and D_H at that point when T_e changes. As a fixed point it is appropriate to take the point of Δr= -3.5cm because it experiences the diffusion by D_{KP} before the transition and by D_H after that. As pointed in the previous section, D_{KP} and D_H can be written as $D_{KP}=C_{KP}T_e^{5/6}$ and $D_H=C_HT_e^{-2}$. At Δr=-3.5cm, D_{KP}, D_H and T_e can be read from Fig. 2(b), Fig. 2(c) and Ref.(10) in case of both L and H mode. Therefore C_{KP} and C_H can be fixed easily in both cases. Finally, D_{KP} and D_H can be obtained as a function of T_e. The results are shown in Fig. 3 where the actual points in L and H mode corresponding to Fig. 2(b) and Fig. 2(c) respectively are marked by L and H. Therefore, at the L-to-H transition, L point is found to move to H point through some passages. TL point represents the point where D_{KP} becomes equal to D_H in L-mode state, corresponding to the point with T_{th} expressed by Eq.(14). Similarly, TH point represents the point where D_{KP} is equal to D_H in H-mode state.

With the use of Fig. 3, let's try to make the behavior of the transition clearer. If some temperature rise occurs to exceed $T_{th}(L\to H)$, L points moves over TL point and the dominant diffusion changes from D_{KP}^L to D_H^L and decreases along the D_H^L line unless the density, the density gradient and other parameters are changed. L point never reaches H point. If some change of n_e or dn_e/dr occurs, it becomes possible to make C_H decrease and D_H^L line reach D_H^H line.

In case of H-to-L transition, the similar process is likely to be speculated. That is, if temperature decrease occurs to exceed $T_{th}(H\to L)$, H point moves to TH point, and if it accompanies some change of $n_e(r)$ or some other parameters to make C_{KP} increase to reach D_{KP}^L line, TH point moves to L-point.

Here an important condition for the transition that a large change of plasma parameters, especially density gradient, which is found very effective by the term $\theta^{10/3}r_n$ in Eq.(11) because θ contains r_n linearly, should occur at the transition. If it does not occur, L-point moves along D_{KP}^L until it reaches TL point, then it only goes down along D_H^L line, which results in no improvement of the diffusion coefficient around $T_e\simeq$470eV, compared with L-point. Therefore, some mechanism which may enhance the change of the density profile should be expected at the temperature change at the transition.

In the next section, the analysis as to this question is tried.

4. Analysis of L-H transition

In the first place, we set the temperature rise

$$T_e = T_{eo}(1 + \gamma t) \tag{15}$$

where γt is assumed to be small enough not to change the other parameters. Then D_H can be written as

$$D_H = C \cdot \frac{n^{5/3}}{r_n^{13/3} T_{eo}^2} \cdot (1 + \gamma t)^{-2} \tag{16}$$

$$\equiv D_o (1 + \gamma t)^{-2} . \tag{17}$$

To focus our attention to the sudden change of density profile at the transition, we assume the other variables ($T_e(x)$, $Z_{eff}(x)$ etc.) except $n_e(x)$ and $r_n(x)$ to be constant.

Starting point (t=0) should be chosen at the point just over TL point where the diffusion is dominated by D_H, because the condition of the L-to-H transition should be satisfied.

Then, the continuity equation is

$$\frac{\partial n}{\partial t} = - \frac{\partial \Gamma}{\partial x} + S \tag{18}$$

where

$$\Gamma = - D \frac{\partial n}{\partial x} \tag{19}$$

Γ: particle flux density and S: particle source.
Here, to simplify the situation, the continuity equation is taken as one-dimensional and a convective component in Γ is excluded. Then, Eq.(18) can be rewitten as

$$\frac{\partial n}{\partial t} = B(1 + \gamma t)^{-2} + S \tag{20}$$

where

$$B = \frac{\partial D_o}{\partial x} \frac{\partial n}{\partial x} + D_o \frac{\partial^2 n}{\partial x^2} \tag{21}$$

Remembering $\gamma t \ll 1$ and that the time scale interested here (Δt) is so small as n and S, appearing in the right hand side of Eq.(20), does not change in Δt, we treat n and S in the right hand side of Eq.(20) independent of t and seek the solution of $n(x,t)$ through $\partial n/\partial t$ in the left hand side of Eq.(20). That is, in order to solve Eq.(20) approximately we use the iteration method which is only valid in the small time scale Δt. After the time Δt passes by, we may substitute the solution of Eq.(20) at $t=\Delta t$ into the right hand side as an initial value.

Then we set the initial condition as follows;

$$\frac{\partial n}{\partial t} = 0 \tag{22}$$

at t=0 at all the region considered here (in the present case, a few centimeter region of the plasma circumference). Then,

$$B + S = 0 \tag{23}$$

and

$$\frac{\partial B}{\partial x} + \frac{\partial S}{\partial x} = 0 \tag{24}$$

are induced.

With the use of Eqs.(23) and (24), $n(x,t)$ is easily obtained,

$$n(x,t) = \left(\frac{B}{1+\gamma t} + S \right) t + n(x,o) \tag{25}$$

$$\equiv \Delta n(x,t) + n(x,o) \tag{26}$$

and r_n also can be written

$$r_n(x,t) = -n \frac{\partial x}{\partial n} = r_n(x,o) \left\{ 1 + \left(\frac{B}{1+\gamma t} + S \right) \frac{t}{n(x,o)} - \frac{\left(\frac{1}{1+\gamma t} \frac{\partial B}{\partial x} + \frac{\partial S}{\partial x} \right) t}{\frac{\partial n(x,o)}{\partial x}} \right\} \tag{27}$$

$$\equiv r_n(x,o) + \Delta r_n(x,t) \ . \tag{28}$$

And $D_H(x,t)$ can be linearized in the small change of $n(x,t)$ and $r_n(x,t)$ as

$$D_H(x,t) = D_o \left\{ 1 + \frac{5}{3} \frac{\Delta n}{n(x,o)} - \frac{13}{3} \frac{\Delta r_n}{r_n(x,o)} \right\} (1+\gamma t)^{-2} \tag{29}$$

Substituting the results of Eqs.(26) and (28) into Eq.(29) and using the condition of Eqs.(23) and (24), we obtain

$$D_H(x,t) \cong D_o \left\{ 1+\gamma t^2 \left(\frac{8B}{3n(x,o)} - \frac{13}{3} \frac{\partial B/\partial x}{\frac{\partial n(x,o)}{\partial x}} \right) \right\} (1+\gamma t)^{-2} \tag{30}$$

$$\equiv D_o \{1+\gamma t^2 F\}(1+\gamma t)^{-2} \tag{31}$$

where

$$F = \frac{8B}{3n(x,o)} - \frac{13}{3} \frac{\partial B/\partial x}{\partial n(x,o)/\partial x} \quad . \tag{32}$$

Equation (31) tells that the decrease of $D_H(x,t)$ caused by Te-rise represented by the term of $(1+\gamma t)^{-2}$ is enhanced if F is negative, on the contrary, it is weakened if F is positive.

In L-mode plasma, the diffusion coefficient is generally a monotonously increasing function of x, and the density distribution is a monotonously decreasing function of x. At t=0 which we chose at the point just over the threshold temperature $T_{th}(L \to H)$, D and n profiles still remain L-mode-like. Therefore, D_o, $\partial D_o/\partial x > 0$, and $\partial n(x,o)/\partial x < 0$ are easily expected. As for $\partial^2 D/\partial x^2$, $\partial^2 n/\partial x^2$, and $\partial^3 n/\partial x^3$, the physical perspective in general cannot be available easily. But $\frac{\partial^2 D}{\partial x^2} > 0$, $\frac{\partial^2 n}{\partial x^2} < 0$ and $\frac{\partial^3 n}{\partial x^3} < 0$ are very plausible conditions in the plasma circumference of Tokamak. At least the data of Fig. 1(b) in Ref. (10) and Fig. 2(b) fit the case. Therefore, both B and $\partial B/\partial x$ are expected to be negative at t=0, which leads the value F also negative. To summarize the discussion above, at least we can point the possibility that there exists the mechanism which enhances the decrease of the diffusion coefficient at the threshold temperature as T_e increases, though the analysis described here should be reinforced both by the more precise computer calculation and by the more detailed experimental data in the future.

Next, let's move to the case of the H-to-L transition. The temperature decrease can be expressed as

$$T_e = T_{eo}(1 - \gamma t) \quad . \tag{33}$$

A similar procedure as the case of the L-to-H transition can be applied. The initial point is taken at the point of just lower

temperature than $T_{th}(H\to L)$ of Fig. 3. Then, D_{KP} can be written as

$$D_{KP} = C \cdot \frac{n^{1/3} T_{eo}^{5/6}}{r_n^{4/3}} (1-\gamma t)^{5/6} \tag{34}$$

$$\equiv D_o (1-\gamma t)^{5/6} \tag{35}$$

After following the same procedure as the case of the L-to-H transition, D_{KP} can be written as

$$D_{KP} = D_o \left\{ 1 - \frac{5}{12}\gamma t^2 \left(\frac{B}{n(x,o)} - \frac{4}{3} \frac{\partial B/\partial x}{\partial n(x,o)/\partial x} \right) \right\} (1-\gamma t)^{5/6} \tag{36}$$

$$\equiv D_o \{1 - \frac{5}{12}\gamma t^2 G\}(1-\gamma t)^{5/6} \tag{37}$$

where

$$G = \frac{B}{n(x,o)} - \frac{4}{3} \frac{\partial B/\partial x}{\partial n/\partial x} \quad . \tag{38}$$

Contrary to the L-to-H transition, the situation is complicated. In the first place, the radial profile of the diffusion coefficient is not a monotonous function, but it has a possibility of a deep dip as shown in Fig. 2(c). In the second place, Eq.(37) indicates that if G is positive, the decrease of D_{KP} is enhanced, but if G is negative, the decrease of D_{KP} is weakened or D_{KP} may increase if G is negative enough to make the other terms except D_o in Eq.(37) larger than unity. This fact means that the simple enhancement mechanism raising the diffusion coefficient from D_{KP}^H line to D_{KP}^L line of Fig. 3 cannot exist as long as γ is positive. If γ is negative which means the case of the increase of temperature, though that is unlikely to be conceivable because the initial point which is just lower than $T_{th}(H\to L)$ moves back to D_H line when T_e increases, then the enhancement mechanism of D_{KP}-increase exists only when G is positive. In the third place, the dominant diffusion is possibly not only D_{KP} even if electron temperature decreases below the threshold value $T_{th}(H\to L)$, but the diffusion by other instabilities like D_{TE} as shown in Fig. 2(c) may be dominated. If so, the above discussion should take into account the contribution by other instabilities. Therefore, after all, the case of the H-to-L transition is too complicated

to draw out some conclusion by the present simple analysis. (Recently discovered improved L-mode[11] may be speculated as a result of this complicated situation.)

To conclude the above discussions, it can be shown that the decrease of the diffusion coefficient can be enhanced by the change of n_e and r_n at the L-to-H transition (especially the term $r_n^{13/3}$ in D_H is effectively contributed) and the behavior is schematically shown in Fig. 4, while in the case of the H-to-L transition, it is only said that the situation is too complicated and requires the precise computer calculation. It can be also indicated that the sudden change of the density profile at the L-to-H transition may result from the fact that n_e or r_n dependence on the diffusion coefficient is greatly different between D_{KP} and D_H, so that the density profile which is stable before the transition or below the threshold temperature, turns unstable when T_e increases over the threshold and the dominant diffusion turns D_H.

In the end of this section, it should be noted that the present analysis is a crude sketch of L-H transition merely in order to draw the physical picture, therefore, the more precise analysis should be performed by using the computer calculation, including various types of instabilities and the transport equations as well as the continuity equation.

5. Discussions

In this section, various aspects of L-H transition are investigated on the basis of the model described above. At first surveyed are the ways how the H-mode can be achieved easiest, with the use of the knowledges developed on the model. Easily understandably it is advantageous to make the temperature threshold as low as possible. Equation (14) informs us of the prescription to make lower the values of a, B, Z_{eff}, and n_e, and higher the values of A, r_n, r, and Ip. But, B/Ip cannot be easily changed because of keeping the appropiate q-value. Therefore, in the first place, q-value should be low as long as a plasma is stable. If we approximate r~a (it's no problem because the situation here is limited at the circumference). T_{th} is found approximately proportional to $a^{44/17}$, so that T_{th} eventually becomes proportional to $a^{10/17}$ approximately when the fact that $q_a \propto a^2$ and q_a is fixed now is taken into account. This fact tells that a small minor radius (a) makes T_{th} low. As for a current density profile, we can easily conclude from Eq.(14) the advantage of a flat profile. With regard to n and r_n, remembering Eq.(2), it is found that a low density gradient (a flat profile) and a high density are preferable. Concludedly, the prescription is that low a, low Z_{eff}, low q, large A, high n and flat profiles of particle density and current density are preferable. Here, let's try to compare T_{th} in Eq.(14) of the actually operating machines. To do that, the following assumptions are necessary not only to supply unknown factors but to give the equal basis for the comparison: $r_n = \frac{1}{5}a$, $j=j_o(1-r^2/a^2)$, $T_i=T_e$, $\eta_e=1$, $n_e=1\times10^{19}$ m^{-3}, $Z_{eff}=2$, A=2, and r=0.9a. The results are shown in Table 1, which tells the interesting fact that JT-60 and ASDEX show high values while JET, DIII-D and JFT-2M show low values. As for JT-60, it is consistent with the fact that JT-60 is difficult to get H-mode. JT-60 uses hydrogen gas in the actual experiment, so that T_{th} goes up to ~590 eV if A=1. From Table 1, this value is found over twice of that of JET. As for ASDEX, the question occurs why ASDEX can get H-mode so easily while JT-60 cannot. The answer will be prepared in the following paragraph as to the lower limit of density for H-mode. The question why T_{th} of JET et al. is much smaller than that of ASDEX and JT-60 can be easily answered by the fact that JET et al. is noncircular and able to make B much smaller than ASDEX and JT-60. It

should be noted here that the discussions in the second section do not include the noncircularity, but the theory is based on the slab model so that the effect of noncircularity may be small, though the precise analysis is left as a future task.

In the actual experimental situation, the profiles of both particle density and current density cannot be easily controllable, and the machine parameters (a,R) cannot be largely changeable. Therefore, not so many means to lower the threshold are left. The comparatively easily obtainable ways will be as follows; to use a heavier atom, to make a minor radius (a) as low as permissible, to lower Z_{eff} by changing wall conditions (wall component, wall temperature, the distance between plasma and wall), to raise NBI power, to use ECH for the effective heating for electrons at the circumference, to make a plasma shape noncirculer to get a lower B, or to do something to make the electron temperature near the plasma edge prone to rise. For the purpose listed here in the last (as it were, to make T_e rise), often tried is to lower the plasma density. But it is found not so wise because T_{th} of Eq.(14) is proportional to $n^{-10/17}$ (which is easily found if Eq.(2) is used), that is, T_{th} also goes up if you lower n, with the conditions that the other parameters are unchanged. Furthermore the experiments[6] tell that the lower limit of the plasma density exists for obtaining H-mode.

Now, let's try to find whether the lower limit of the density exists or not according to our model. As a necessary condition for the L-to-H transition, we should remember that there are two conditions that the dissipative drift wave must be dominant near the plasma circumference and electron temperature must exceed T_{th} given by Eq.(14). Therefore, the competitive candidates of the instabilities should be low enough not to influence the dominant diffusion. What are the possible candidates? At first, the collisionless drift wave should be taken into account. After careful numerical ordering, this effect is found low enough. The most plausible candidate is the dissipative trapped electron mode, especially in case of a low density. In order to make the dissipative trapped electron mode negligible, the effective collision parameter $\nu_e^*=\nu_e qR/\varepsilon^{3/2}v_e$ should be larger than unity. Using the same assumptions when Eq.(14) is induced, this condition can be rewritten as

$$T_e(\mathrm{eV}) \leq 1.68\times10^{-5}\ \frac{Z_{eff}^{1/2} n_e^{1/2} B^{1/2} r^{1/2}}{Ip^{1/2}\frac{r}{a}[1-\frac{r^2}{2a^2}]^{1/2}\varepsilon^{1/4}} (\equiv T_{th}^{TE}) \tag{39}$$

where the unit of the right hand side is MKS unit.
Therefore, T_e should satisfy the conditions of both Eq.(14) and Eq.(39) for the L-to-H transition. As it were, there must exist some region near the plasma edge where T_e is larger than T_{th} as well as smaller than T_{th}^{TE}.

For the sake of that, therefore, the condition of

$$T_{th} \leq T_{th}^{TE} \tag{40}$$

is needed at that region. Therefore it should be concluded that if Eq.(40) is not satisfied at any region near the plasma edge, the L-to-H transition cannot be achieved even if you raise T_e extremely near the plasma edge because the dominant diffusion is forced to be taken place by the dissipative trapped electron mode and our model cannot be applied.

Equation (40) can be rewritten as

$$n_e^{1/36} r_n \geq 6.74\times10^2\ \frac{B^{19/36} a^{41/9}\{\frac{r}{a}[1-\frac{r^2}{2a^2}]^{1/2}\varepsilon^{1/4}\}^{17/18}(1+\eta_e)^{1/3}}{Z_{eff}^{1/36} A^{5/18} Ip^{5/12} r^{59/36}(1+\frac{Ti}{Te})^{1/9}} . \tag{41}$$

If we set $n_e \equiv \alpha\times10^{19}\ \mathrm{m}^{-3}$, Eq.(41) is given as

$$\alpha^{1/36} r_n \geq 1.44\times10^2 \frac{B^{19/36} a^{35/12} \varepsilon_a^{17/72}(1+\eta_e)^{1/3}}{Z_{eff}^{1/36} A^{5/18} Ip^{5/12}(1+\frac{Ti}{Te})^{1/9}} (\equiv r_n^{th}) \tag{42}$$

or

$$n_e \geq 1.44\times10^2\ \frac{B^{19/36} a^{35/12} \varepsilon_a^{17/72}(1+\eta_e)^{1/3}\left|\frac{dn_e}{dr}\right|}{Z_{eff}^{1/36} A^{5/18} Ip^{5/12}(1+\frac{Ti}{Te})^{1/9}} (\equiv n_{th}) \tag{43}$$

where approximately we can set r=a and $\alpha^{1/36}\simeq1$ because $\alpha^{1/36}$ varies only 0.94~1.07 even if α varies between 0.1~10. Therefore, Eq.(43) should represent the lower limit of plasma density at the L-to-H transition. Here, to try to investigate the validity of Eq.(42) or

(43) numerically, we use the parameters in Table 1 to obtain r_n^{th} of each machine as follows; $r_n^{th} \cong 0.32$m (JET), ~0.34m (JT-60), ~0.052m (ASDEX), ~0.079m (DIII-D), and ~0.02m (JFT-2M) respectively. Except JET and JT-60, those are all favorable values because the values are found below ~1/6 of the minor radius (a) of each machine. That is very plausible. As for JT-60, for example, the fact that r_n^{th} ~0.34m means that r_n must be larger than r_n^{th} ~0.38a near the plasma edge. That is an unlikely situation in L-mode plasma before the transition. Therefore, JT-60 is proved to be a difficult machine to attain H-mode even in this respect. As for ASDEX, the fact that r_n^{th}~0.052m~0.13a means that it has enough r_n to spare, in other words, it is able to lower the density enough to obtain H-mode. As for JFT-2M it can be said that this device is the easiest machine to obtain H-mode in this respect. As another favorable proof of the present analysis there is the fact that n_{th} of Eq.(43) is proportional to $B^{19/36}$ which is supportive with the experimental result of JET[6] ($n_{th} \sim 2\times10^{19}$ m^{-3} at B=2.2T and $n_{th} \sim 3\times10^{19}$ m^{-3} at B=3-3.5T), if we take into account that the density gradient, appearing in Eq.(43), empirically becomes steeper as B is made stronger.

After the L-to-H transition, ν^*_{eff} grows smaller than unity so that the dissipative trapped electron mode cannot be ignored, as described in the previous section and the effect also shown in Fig. 2(c), where it is steeply growing around $\Delta r \cong -3$cm, and the deep dip, combined with D_{TE} and D_H, is formed, which may lead to the flat profile or pedestal of density, and electron temperature, too, through χ_e related with the diffusion coefficient. But it should be noted here that the deep dip is essential for our model, as described in the previous sections, but even around $\Delta r \simeq -3.5$cm where D_{TE} still remains at a comparatively low value, ν^*_{eff} already grows smaller than unity so that D_{TE} should have had a much larger value round $\Delta r \simeq -3.5$cm and it should have led the vanish of the deep dip. But it is not the case because R/r_n, which is very effective in damping D_{TE} if it is larger than ~8, becomes larger than ~8 in the region of $\Delta r \gtrsim -3.5$cm. Therefore, the deep dip can be formed around this narrow region of ~1.5 cm around $\Delta r \simeq -3.5$cm, though it may vanish if D_{TE} dominates all around the region.

If our model, which is mostly limited in the circumference of a plasma, were accepted, then how should the experimental result of the improvement of the heat conduction in the inner part of a plasma be

explained? In H-mode plasma, Fig. 2(c) shows the characteristic feature of a deep dip of the diffusion coefficient and in the previous section, the increase of Δr_n is shown to enhance the transition. Therefore, it can be said that the deep dip works as though the particle flow or the heat flow, diffused from the inner part, stops at this well to induce the decrease of the density gradient (the increase of r_n) of the inner part of the plasma to finally result in the flat profile. If the inner part of the plasma is dominated by the dissipative trapped electron mode, the increase of r_n gives the favorable effect to improve the heat conduction, though it gives the unfavorable one if it is dominated by η_i-mode. Which modes or other possible modes are dominant has not been made fully clear as yet. Therefore, the question here also cannot but remain as a future task.

6. Conclusions

To summarize the results:

1) It is shown that the dissipative drift wave turbulence can be a main actor of L-H transition, and the cause of the transition is the change of the dependence of the plasma parameters on the diffusion coefficient at $k_\perp \rho_i = 1$. Especially the dependence of electron temperature changes from $T_e^{5/6}$ to T_e^{-2} at $k_\perp \rho_i = 1$ as electron temperature increases.
2) The threshold of electron temperature for the transition is given and compared with the experimental results to show the good agreement as to both the value and parameter dependences.
3) The presented model is applied to the experimentally obtained n_e and T_e profiles of ASDEX, and, it is shown that the model fits the data by confirming that the expected threshold appears in H-mode plasma and does not appear in L-mode plasma.
4) It is shown that the diffusion coefficient profile of H-mode has a deep dip formed by D_H with a low value, combined with another instability with a large value, for which we take the dissipative trapped electron mode as a most plausible candidate. This deep dip is shown to be able to take a part in the good confinement of the inner part of H-mode plasma.
5) The physical picture is given that the increase of electron temperature at the L-to-H transition enhances the increase of n_e and r_n which furthermore enhances the decrease of D_H owing to both the term $r_n^{-13/3}$ and the radial profiles of both the diffusion coefficient and the density which still have a L-mode-like form.
6) The expected procedures from the model to obtain H-mode are discussed and the threshold values for the various Tokamak decices are calculated and found to give a reasonable value. The reason on the difficulities to obtain H-mode by JT-60 is revealed. The advantage of noncircularity is also shown.
7) The lower limit of density to obtain H-mode is induced by using the effective collision parameter of the dissipative trapped electron mode, showing the reasonable values of the various divices, when applied to the Tokamak machines.

It should be noted in the end that the precise experiments to obtain the detailed distribution profiles of n_e, j, Z_{eff}, T_i, T_e and so on are expected to prove the model definitely.

Acknowledgement

To study the present theme, it was a crucial point for the author to experience the H-mode experiment on the spot. Fortunately, the author could have the opportunity to participate in D-III experiment in 1982 in which the H-mode discovery was tried and succeeded just one month after the presentation of H-mode discovery by ASDEX at the IAEA conference in Baltimore. I would like to express the appreciation not only to the superiors at that time of our institute who gave the author the opportunity, but also to D-III members who did me a favor of the various discussions.

The author might as well thank the JT-60 team, because the fact that JT-60 has suffered a long time to struggle to obtain H-mode is also one of the motivations of this study.

In the last place, the author expresses the gratitude to Dr. Iijima, Dr. Shirakata, Dr. Maeda and Dr. M. Tanaka who helped to move the author to the present division to give the time to study the present research.

References

1) F. Wagner et al.; in Proc. 9th Inter. Conf. on Plasma Phys. and Cont. Nucl. Fusion Research, Baltimore, U.S.A., 1-8 Sep.,('82) vol.I, P43

2) A. Kitsunezaki et al., in Proc. 10th Inter. Conf. on Plasma Phys. and Cont. Nucl. Fusion Research, London, 12-19 Sep., ('84) vol.I, P57
A. Tanga et al., in Proc. 11th Inter. Conf. on Plasma Phys. and Cont. Nucl. Fusion Research, Kyoto, 13-20 Nov., ('86), vol.I, P65
K. Odajima et al., in Proc. 11th Inter. Conf. on Plasma Phys. and Cont. Nucl. Fusion Research, Kyoto, 13-20 Nov., ('86) vol.I, P151
and many others

3) F.L. Hinton; Nucl. Fusion 25 ('85) 1457
C.M. Bishop; Nucl. Fusion 26 ('86) 1063
N. Ohyabu, G.L. Jahns, R.D. Stambaugh and E.J. Strait; Phys. Rev. Lett. 58 ('87) 120
S.-I. Itoh and K. Itoh; Nucl. Fusion 29 ('89) 1031
and many others

4) G. Becker; Nucl. Fusion 28 ('88) 1458

5) B.B. Kadomtsev and O.P. Pogutse; Reviews of Plasma Physics vol.V, P249

6) JET team (presented by M. Keilhacker); IAEA-CN-50/A-III-2 in 12th Inter. Conf. on Plasma Phys. and Cont. Nucl. Fusion Research, Nice, France, 12-19 Oct., ('88)

7) N. Suzuki et al.; in Proc. 14th Eur. Conf. on Cont. Fusion and Plasma Heating, Madrid ('87) Part 1, P217

8) K. Toi et al.; in Abstracts of the Autumn Meeting of Physical Society of Japan, Kagoshima, 3-6 Oct. ('89), Part 4, P220, in Japanese

9) T.N. Carlstrom, M. Shimada, K.H. Burrell, J. DeBoo, P. Gohil, R. Groebner, C. Hsieh, H. Matsumoto, and P. Trost; in Proc. Eur. Conf. on Cont. Fusion and Plasma Physics, Venice, 13-17 Mar. ('89), Part 1, P241

10) K. Lackner et al.; in Proc. 10th Int. Conf. on Plasma Physics and Cont. Nucl. Fusion Research, London, 12-19 Sep. ('84) vol.I, P319.

11) M. Mori et al.; in Proc. Eur. Conf. on Cont. Fusion and Plasma Physics, Venice, 13-17 Mar. ('89), Part 1, P213

Table 1 The threshold values (T_{th}) of the Tokamak devices, calculated from Eq.(14).

Devices / Threshold Temperature	JT-60	JET	DIII-D	ASDEX	JFT-2M
	a = 0.9 m R = 3.0 m B = 4.5 T Ip = 2.8 MA	a = 1 m R = 2.8 m B = 2.2 T Ip = 3 MA	a = 0.55 m R = 1.7 m B = 2.1 T Ip = 1.2 MA	a = 0.4 m R = 1.6 m B = 2.2 T Ip = 0.32 MA	a = 0.3 m R = 1.3 m B = 1.2 T Ip = 0.2 MA
T_{th} (eV)	~ 480	~ 250	~ 220	~ 500	~ 270

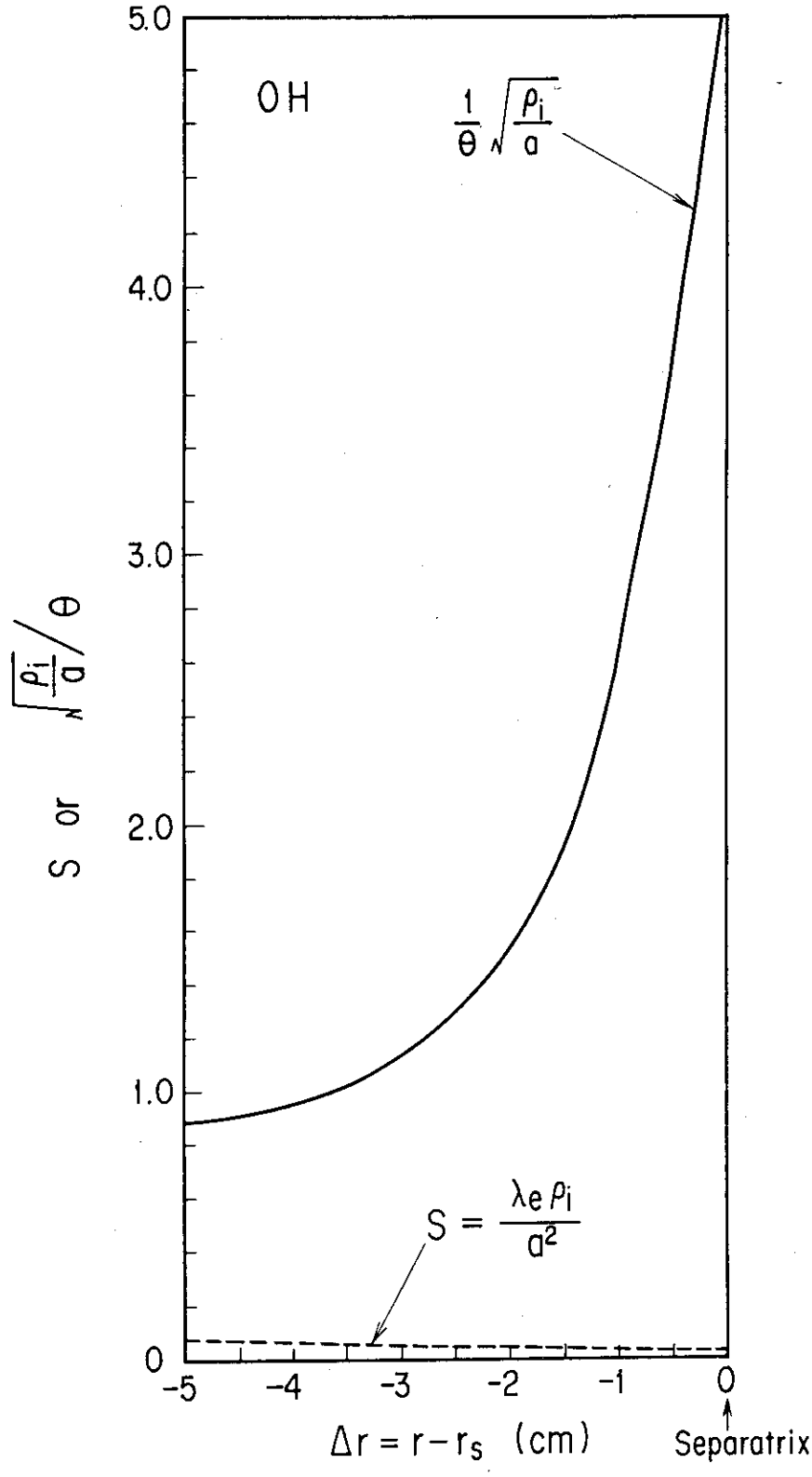

(a)

Fig. 1 The calculated results of a collisional parameter $S(=\lambda_e \rho_i/a^2)$ and $\sqrt{\rho_i/a}\,/\,\theta$, based on the data of Ref.(10) in case of (a) Ohmic plasma, (b) L-mode plasma, and (c) H-mode plasma.

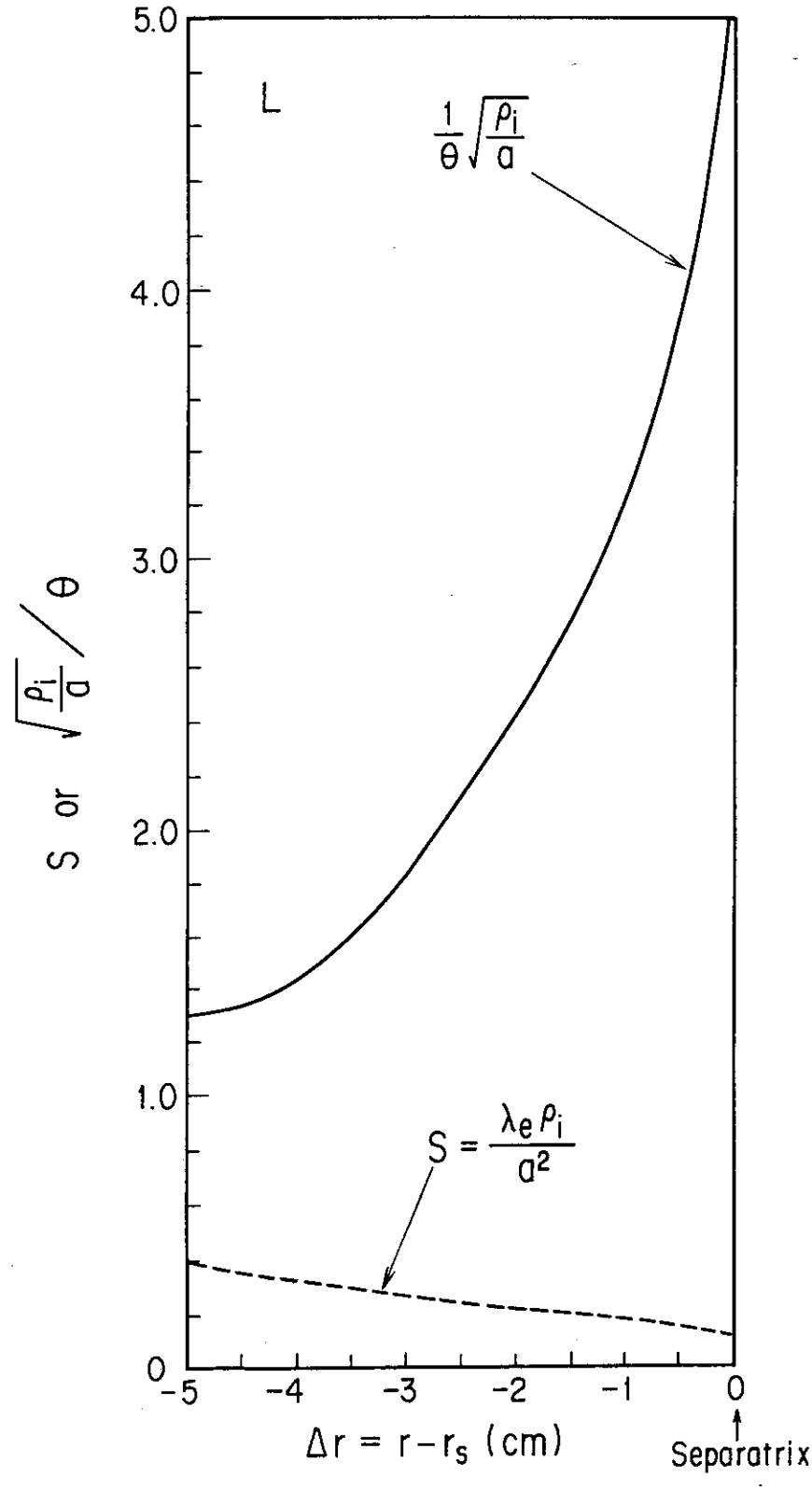

(b)

Fig. 1 (Continued)

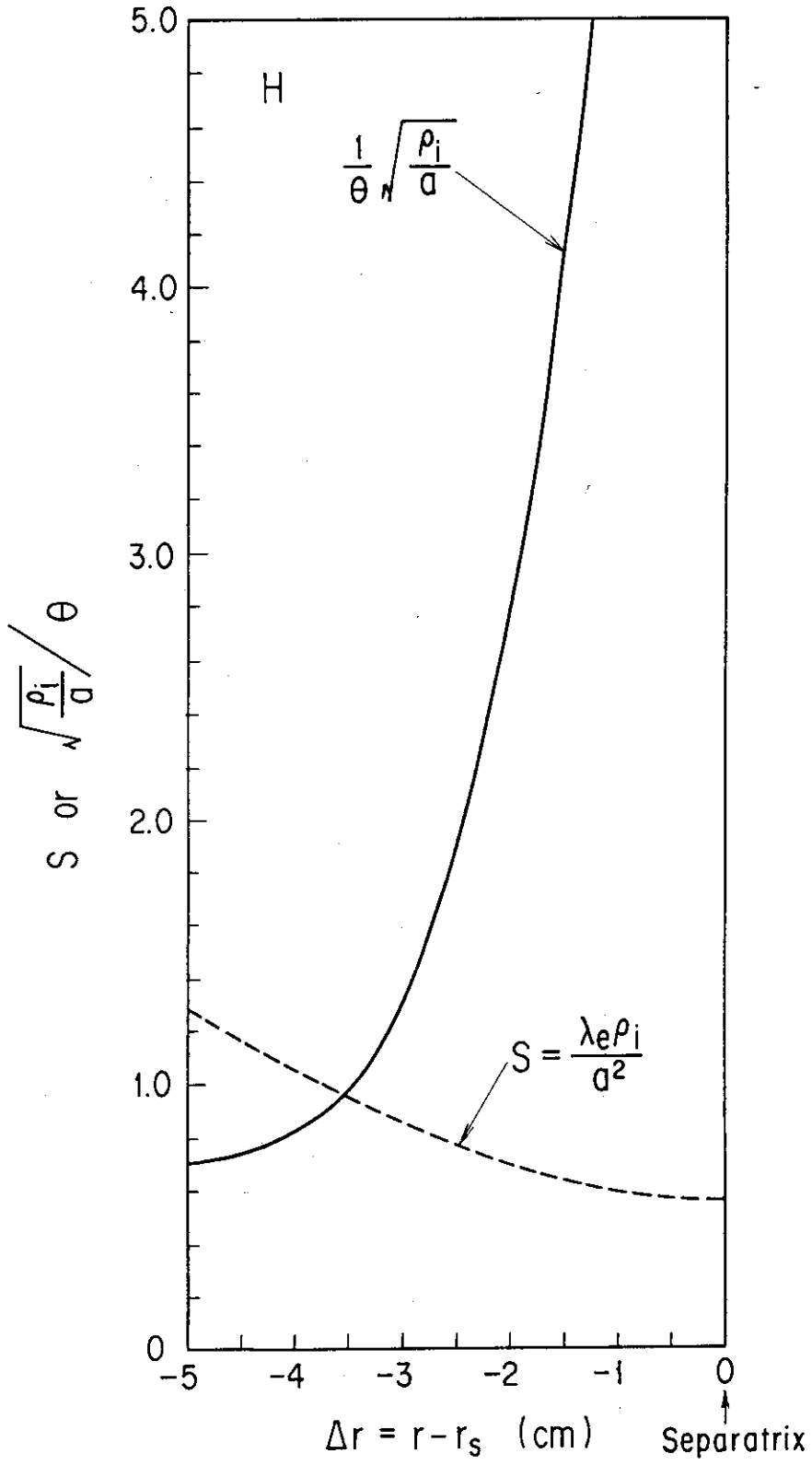

(c)

Fig. 1 (Continued)

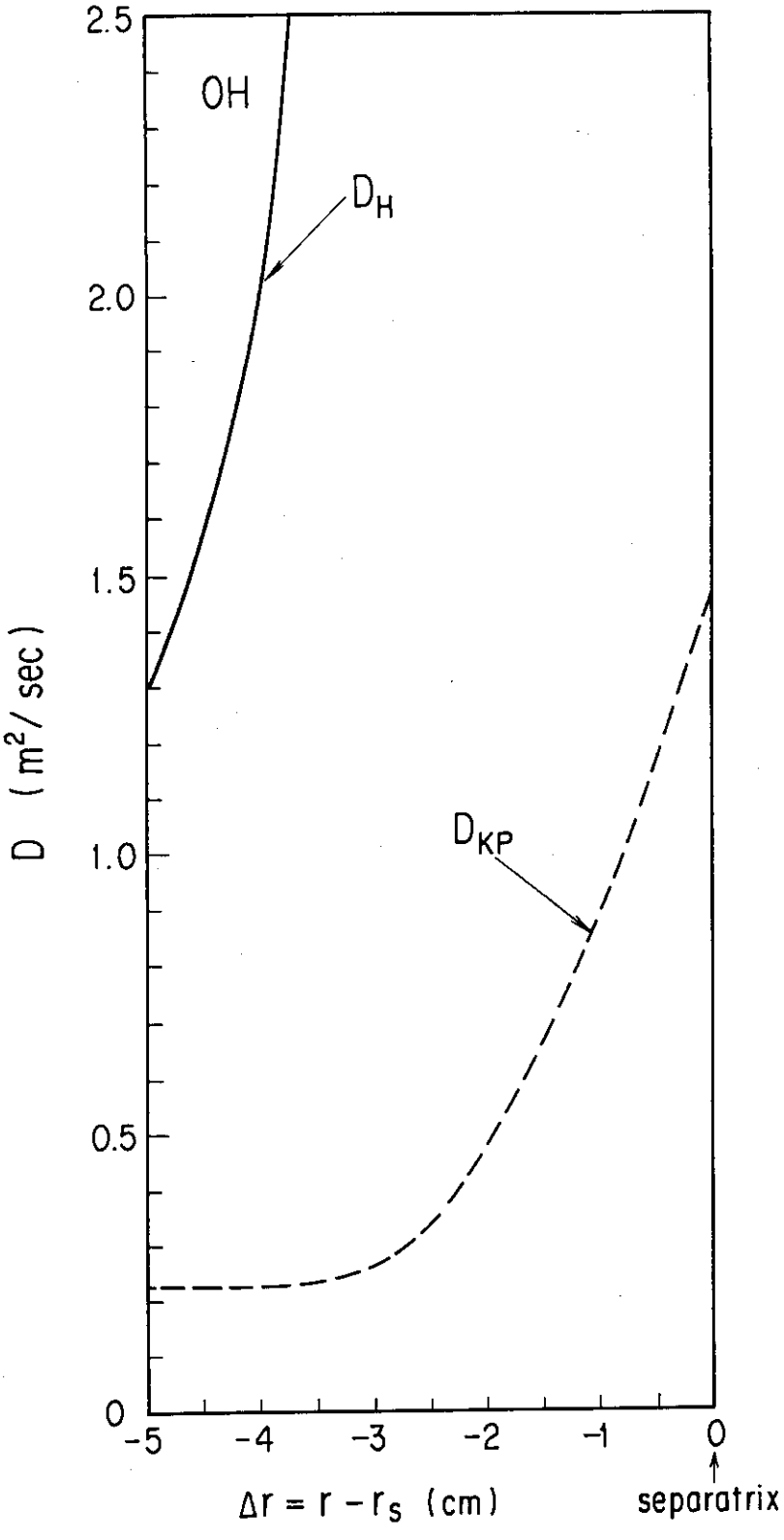

(a)

Fig. 2 The calculated results of the diffusion coefficient D_{KP} and D_H, based on the data of Ref.(10) in case of (a) Ohmic plasma, (b) L-mode plasma, and (c) H-mode plasma. (In Fig. 2(c), the diffusion coefficient D_{TE} due to the dissipative trapped electron mode is added)

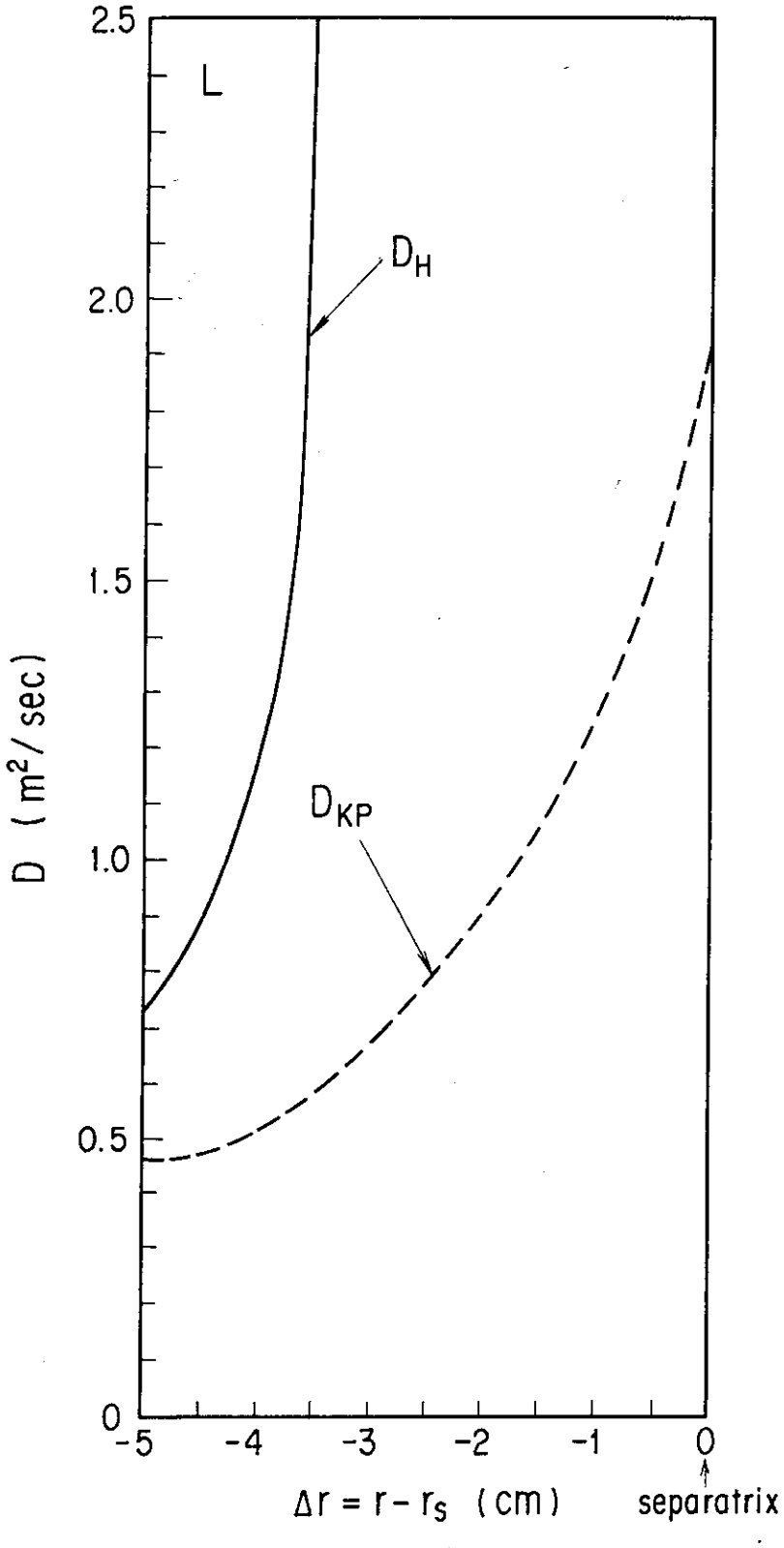

(b)

Fig. 2 (Continued)

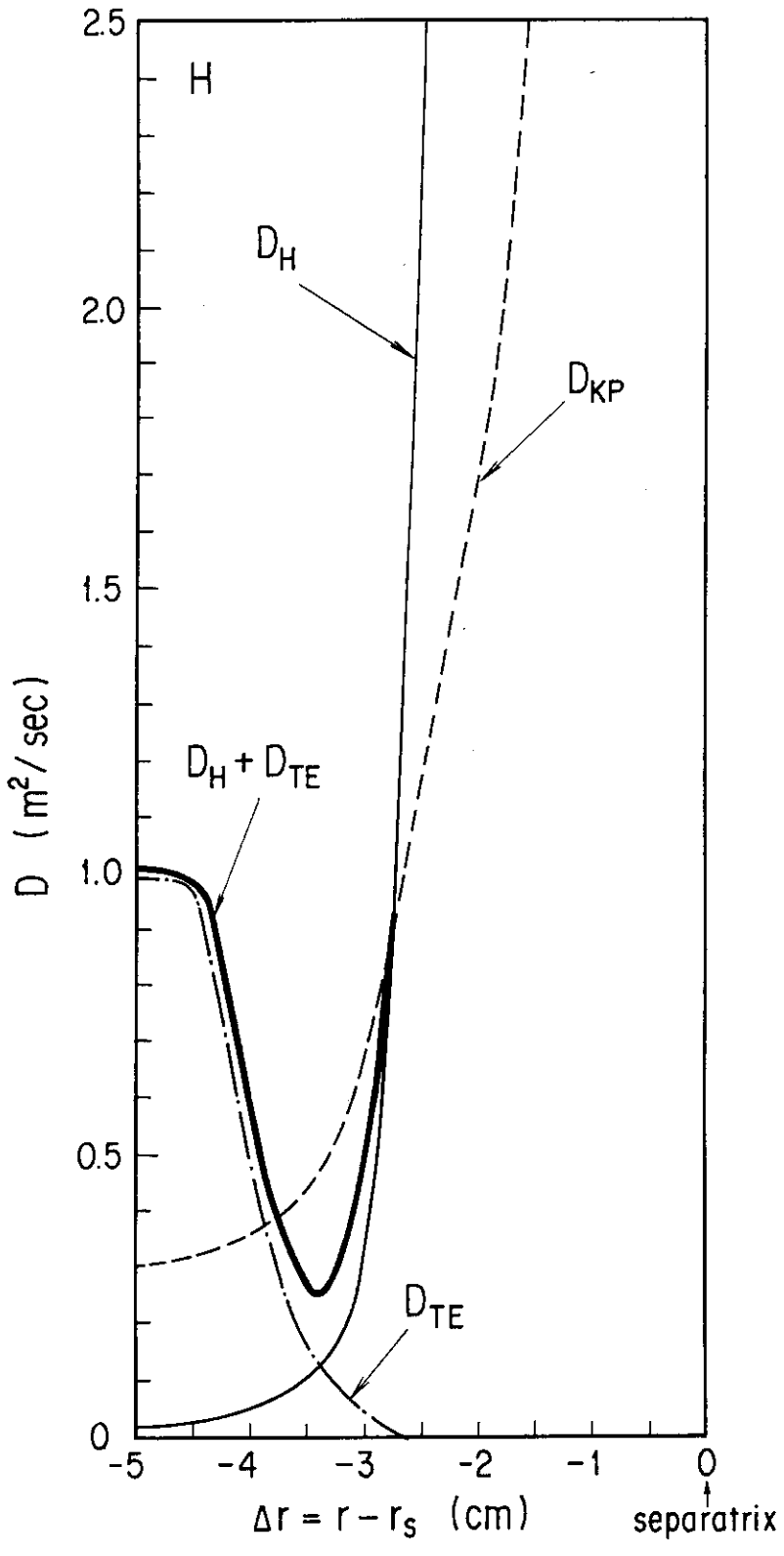

(c)

Fig. 2 (Continued)

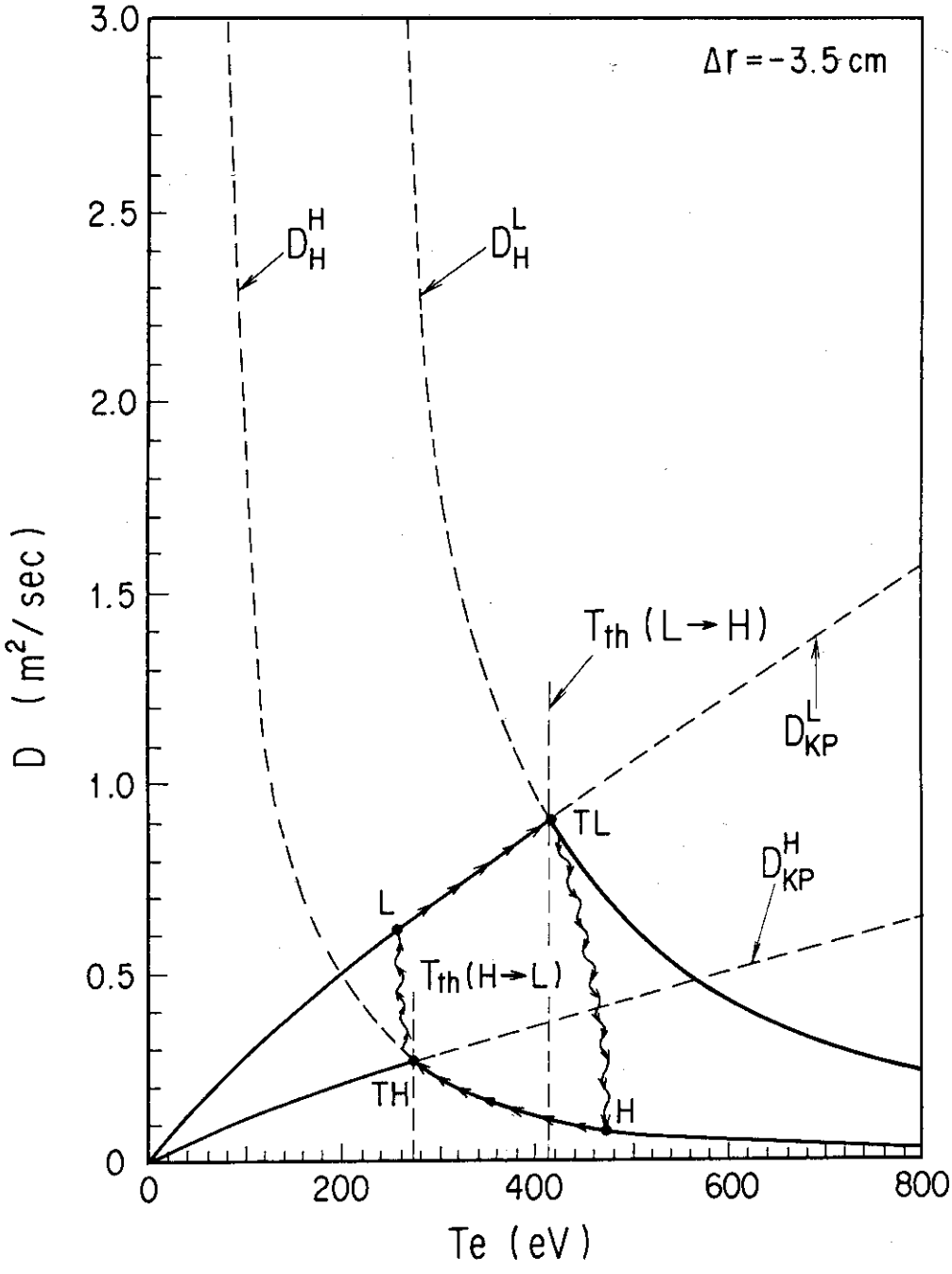

Fig. 3 The diffusion coefficient D_{KP} and D_H as a function of electron temperature (T_e) at Δr=-3.5cm. D_{KP}^L and D_H^L represent the diffusion coefficient D_{KP} and D_H of L-mode plasma respectively, calculated from the data of Fig. 2(b) at Δr=-3.5cm, while D_{KP}^H and D_H^H represent the diffusion coefficient D_{KP} and D_H of H-mode plasma respectively, calculated from the data of Fig. 2(c) at Δr=-3.5cm.

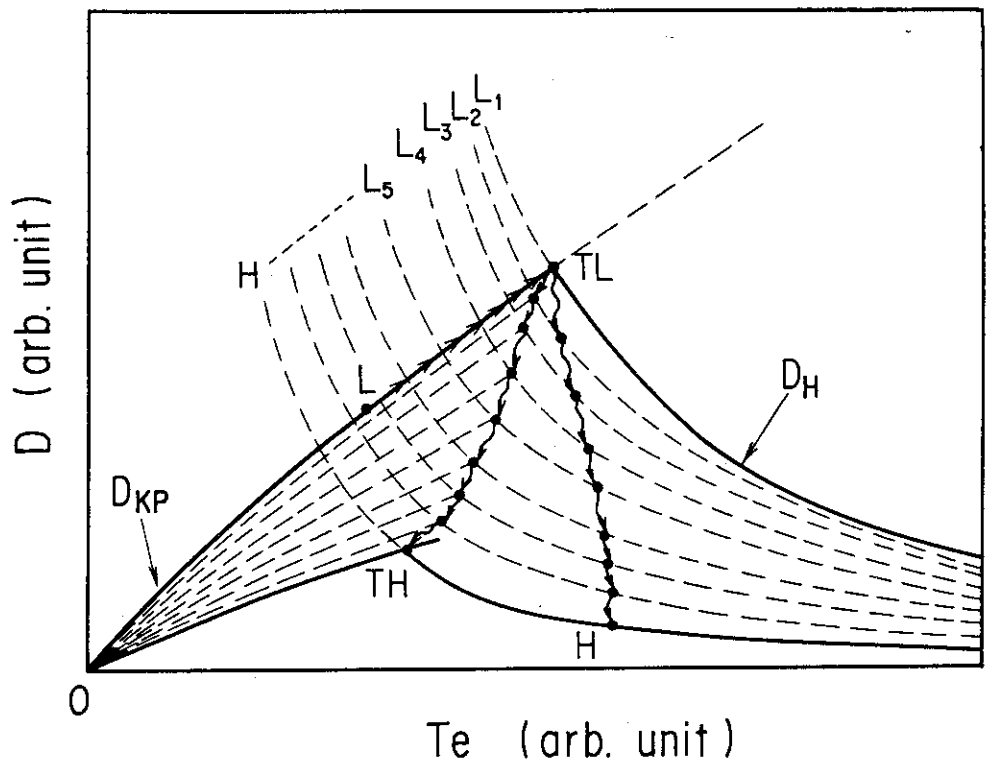

Fig. 4 The schematic behavior of the diffusion coefficient D_{KP} and D_H changing from D_{KP}^L and D_H^L lines to D_{KP}^H and D_H^H lines respectively during the L-to-H transition.